J. Fluid Mech. (1988), *vol.* 188, *pp.* 159–184
Printed in Great Britain

A jet in crossflow

By D. J. NEEDHAM, N. RILEY
School of Mathematics, University of East Anglia, Norwich NR4 7TJ, UK

AND J. H. B. SMITH
Aerodynamics Department, Royal Aircraft Establishment, Farnborough GU14 6TD, UK

(Received 6 May 1987)

The flow of a jet of an inviscid, incompressible fluid emerging from a cylindrical pipe, of circular cross-section, into a stream of the same fluid is considered. The component of the external flow normal to the axis of the pipe is taken to be small compared with the speed of the jet. The results throw some light on the mechanisms that are responsible for the observed deflection of jets into the crossflow direction.

1. Introduction

The behaviour of a jet exhausting into a fluid of similar density which is flowing at an angle to the jet axis (the jet in crossflow) is important in a wide range of situations, from the dispersal of pollutants in the environment to the aerodynamics of aircraft like the Harrier in the transition between wing-borne and jet-borne flight. The present paper treats the mathematical problem that arises from a highly idealized model of flows of this type. The geometry considered is a semi-infinite pipe with vanishing wall thickness, in the form of a right circular cylinder, in an unbounded space. The fluid is assumed to be inviscid and incompressible, with the same density throughout. Far from the pipe the fluid moves with uniform velocity, and within the pipe, far from the orifice, it also moves with uniform velocity. The jet emerges from the orifice bounded by a stream surface common to the interior and exterior flows, across which the pressure is continuous. Without wishing to dismiss the possibility that the appropriate solution may be unsteady, we seek a solution that is independent of time. This takes the form of a pair of potential functions, solutions of Laplace's equation, coupled by conditions on an initially unknown boundary. We do not specify the direction or properties of the jet at a large distance from the origin because the mean streamlines in the jet surface act like characteristics, as discussed in §4, because we believe the disturbance introduced by the jet into the uniform flow at infinity is negligible in three dimensions, and because the analysis we use does not require such downstream boundary conditions. In this way, we obtain a problem which appears well-posed but intractable.

The classical approach of introducing a small parameter is followed. The component of the ambient velocity normal to the axis of the pipe is assumed to be small compared with the velocity in the pipe. The departure of the jet from the circular cylinder defined by the pipe is, consistently, also assumed to be small. The component of the ambient velocity along the pipe axis is not restricted, although conceptual difficulties arise if its sense is opposed to that of the pipe flow. If the normal component of the ambient velocity is ϵ times the undisturbed speed in the pipe, where ϵ is small, we can distinguish two distinct lengthscales in the development

of the jet. The first is obviously the scale of the pipe radius a; the second emerges as the longer scale a/ϵ. It is on the second scale that deflection of the jet or significant distortion of its cross-section takes place. The first few terms in an expansion of the appropriate solution can be found relatively easily. They provide a downstream boundary condition for the solution on the scale of a. A solution on this scale, expressed in terms of integrals, has been obtained, by an application of the Wiener–Hopf technique, as used by Lennox & Pack (1963) for planar, compressible jets.

Before outlining the results obtained, we provide some motivation for this approach to the jet in crossflow. A characteristic feature of the real flow is that the jet path is deflected towards the direction of the ambient flow. A second characteristic feature is that the disturbance field of the deflected jet at a large distance from the orifice is dominated by a pair of contrarotating vortices aligned with the jet. A third characteristic feature is the highly turbulent nature of the flow, arising partly from the instability of laminar shear layers at the high Reynolds numbers typical of the practical occurrences and partly from the unsteadiness of the separation of the ambient flow from the jet surface. In view of the last of these features, and of the more familiar case of the aligned jet, it is clear that any detailed predictive method must be based on a flow model in which Reynolds stresses are represented. Valuable approaches on these lines are those of McGuirk & Rodi (1979) and Sykes, Lewellen & Parker (1986), who also reference other works in the field. Calculations of this kind are, however, of limited value in elucidating the flow mechanisms that are involved in the distortion and deflection process. In principle, Reynolds stresses and viscous stresses could be set to zero in the algorithms used, but numerical instability is then likely to ensue unless substantial numerical damping, with dissipative properties, is present in the calculation. On the other hand, the success of inviscid models of three-dimensional flows involving concentrations of vorticity, from the wing theory of Lanchester and Prandtl onwards, invites attempts to explain the first two characteristic features on an inviscid basis. Many such attempts have been made, starting with the work of Chang (1942), and concentrating on the flow in planes normal to the centreline of the jet. These treatments have been able to account in a qualitative way for the deformation of the jet cross-section along its length, but relating the axial flow to the crossflow is more difficult, and they are unable to predict the deflection of the jet centreline. Moreover, for the fully three-dimensional flow near the jet exit a more elaborate treatment is clearly required.

A further practical incentive to examine inviscid models of the jet in crossflow arises in the aeronautical context, where there is a need to take into account the interaction between the jet, the external shape of the aircraft and the 'ground', where the last may be part of the Earth's surface, the superstructure of a ship, or the wall of a wind tunnel. Practical methods for such ambient flows are still based on the classical aerodynamic model of an inviscid fluid, with boundary conditions modified to take account of boundary-layer effects. Consequently, a jet model which can be incorporated into such a treatment of the ambient flow would be highly desirable. In any case, it is important to know how much of the characteristic behaviour of the jet in crossflow is predictable on an inviscid basis, and how much depends on the representation of tangential stresses.

On the key question of the deflection of the jet, the results of the present investigation are not entirely conclusive. They show that the component of the ambient velocity along the axis of the pipe plays a crucial role. If this is zero, that is to say if the pipe is perpendicular to the ambient flow, the deformation of the jet

is symmetrical fore-and-aft, there is no force on the jet, and there is no deflection of the jet, at least to the number of terms so far calculated. With a non-zero axial component of the ambient velocity, the jet deforms asymmetrically, there is a force on the cross-section of the jet, and the centroid of the jet cross-section is displaced, corresponding to a deflection of the jet. The deflection of the jet is downstream if the component of the ambient flow is in the same sense as the velocity in the pipe, i.e. if the pipe is inclined downstream.

The mathematical problem is formulated in §2. Section 3 contains the first part of the solution, valid for distances of the order of a/ϵ from the orifice, and a summary of the results of the second part of the solution valid close to the orifice. Details of the latter are given in the Appendices. The results are discussed in more detail in §4.

2. The governing equations

The problem we address is that of the flow of an incompressible, inviscid fluid which emerges, with mean speed U_0, from the orifice of a pipe of circular cross-section, radius a, lying along $-\infty < \bar{x} < 0$ (an overbar denotes a dimensional variable). The jet emerges into a stream of similar fluid which has undisturbed speed $U_0(\lambda^2+\epsilon^2)^{\frac{1}{2}}$, where the magnitude of λ is unrestricted, but $\epsilon \ll 1$; the pipe is at an angle $\tan^{-1}(\epsilon/\lambda)$ to the undisturbed stream direction (see figure 1). The flow is assumed to be steady and irrotational throughout. The undisturbed pressure outside the pipe is $\bar{p}_\infty$ and within the pipe, far from its orifice, $\bar{p}_{-\infty}$. We assume that

$$\bar{p}_{-\infty} - \bar{p}_\infty = \tfrac{1}{2}\rho U_0^2(2\alpha - 1)\,\epsilon^2, \tag{2.1}$$

where α is a given constant, and ρ is the fluid density. This assumption of a small difference between the undisturbed jet and stream pressures ensures that the initial departure of the jet shape from a circular cylinder of radius a is small.

Non-dimensional variables are introduced in which a representative length, velocity and pressure are taken as a, U_0 and ρU_0^2 respectively. In cylindrical polar coordinates (r, θ, x), where the centreline of the pipe lies along the negative axis of x and θ is measured from its leeward generator, Laplace's equation for incompressible potential flow is

$$\frac{1}{r}\frac{\partial}{\partial r}\left(r\frac{\partial \Phi}{\partial r}\right) + \frac{1}{r^2}\frac{\partial^2 \Phi}{\partial \theta^2} + \frac{\partial^2 \Phi}{\partial x^2} = 0. \tag{2.2}$$

In (2.2) Φ represents either the velocity potential of the outer streaming flow or of the inner jet flow which are respectively denoted by φ and $\tilde{\varphi}$. The boundary conditions require, at the pipe surface

$$\frac{\partial \varphi}{\partial r} = \frac{\partial \tilde{\varphi}}{\partial r} = 0 \quad \text{on } r = 1, \quad x < 0, \tag{2.3}$$

and at the jet surface, denoted by $F(r, \theta, x) = 0$, $x > 0$,

$$\nabla\varphi \cdot \nabla F = \nabla\tilde{\varphi} \cdot \nabla F = 0 \quad \text{on } F = 0. \tag{2.4}$$

From Bernoulli's equation the dimensionless pressure, inside and outside the jet respectively, is given by

$$\tilde{p} = p_{-\infty} + \tfrac{1}{2}\{1 - (\nabla\tilde{\varphi})^2\}, \quad p = p_\infty + \tfrac{1}{2}\{\lambda^2 + \epsilon^2 - (\nabla\varphi)^2\},$$

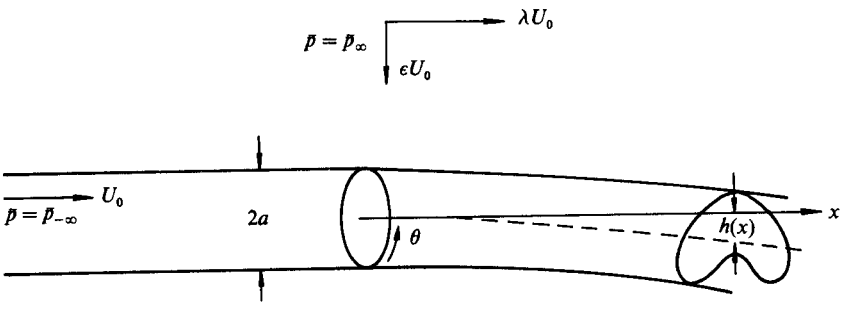

FIGURE 1. Definition sketch.

and continuity of pressure at the jet surface then requires, using (2.1),

$$(\nabla\varphi)^2 - (\nabla\tilde{\varphi})^2 = \lambda^2 - 1 + 2(1-\alpha)\epsilon^2 \quad \text{on } F = 0. \tag{2.5}$$

Finally, the undisturbed conditions require that

$$\tilde{\varphi} \sim x \quad \text{as } x \to -\infty, \quad r < 1, \tag{2.6}$$

and in the outer flow, far from the pipe and the jet,

$$\varphi \sim \lambda x + \epsilon r \cos\theta. \tag{2.7}$$

3. Solution procedure

As a preliminary we note that at leading order the jet surface is simply $r = 1$ and as a consequence the outer solution, correct to $O(\epsilon)$, is

$$\varphi = \lambda x + \epsilon\left(r + \frac{1}{r}\right)\cos\theta \quad \text{for all } x. \tag{3.1}$$

If, for simplicity, we take $\alpha = 0$ then the solution (3.1), and the dynamic condition (2.5) require that the inner solution, for $x > 0$, takes the form

$$\tilde{\varphi} = x - \epsilon^2 x r^2 \cos 2\theta, \tag{3.2}$$

which in turn, from the kinematic condition (2.4), leads to a modified jet shape given by

$$r = 1 - \epsilon^2 x^2 \cos 2\theta. \tag{3.3}$$

Now, (3.2) and (3.3) are not correct in all their details, and not least because (3.1) is correct only to order ϵ. However (3.3) does indicate that this perturbation procedure will fail for $x \gg 1$, specifically when $x = O(\epsilon^{-1})$. This indication motivates the choice of $\xi = \epsilon x$ as a far-field variable, and we find it convenient to develop the solution in the far field before considering the solution close to the orifice, where $x = O(1)$.

3.1. *The far-field solution; $\xi = O(1)$*

If we introduce the variable $\xi = \epsilon x$ the governing equation (2.2) becomes

$$\nabla^2\Phi + \epsilon^2 \frac{\partial^2\Phi}{\partial\xi^2} = 0, \tag{3.4}$$

where ∇^2 denotes the two-dimensional Laplace operator. Guided by (3.1)–(3.4) we expand the outer, stream potential φ, the inner, jet potential $\tilde{\varphi}$ and the jet shape function F, as

$$\varphi = \frac{\lambda\xi}{\epsilon} + \epsilon\lambda\{\varphi_{11}(r,\theta) + \xi\varphi_{12}(r,\theta) + \xi^2\varphi_{13}(r,\theta) + \ldots\} + \epsilon^3\lambda\{\varphi_{31}(r,\theta) + \ldots\} + \ldots, \tag{3.5}$$

$$\tilde{\varphi} = \frac{\xi}{\epsilon} + \epsilon\{\xi\tilde{\varphi}_{12}(r,\theta) + \xi^2\tilde{\varphi}_{13}(r,\theta) + \ldots\} + \epsilon^3\{\tilde{\varphi}_{31}(r,\theta) + \ldots\} + \ldots, \tag{3.6}$$

$$F = r - 1 - \xi^2 f_2(\theta) - \xi^3 f_3(\theta) - \xi^4 f_4(\theta) + \ldots. \tag{3.7}$$

Consider next the boundary conditions. We find it convenient to transfer the kinematic, (2.4), and dynamic, (2.5), conditions at $F = 0$, where F is given by (3.7), to conditions on $r = 1$. Thus, substituting (3.5)–(3.7) into (2.4), and ignoring terms that are smaller than $O(\epsilon\xi^2)$, we have

$$\varphi_{11r} + \xi(\varphi_{12r} - 2f_2) + \xi^2(f_2\varphi_{11rr} + \varphi_{13r} - f_{2\theta}\varphi_{11\theta} - 3f_3) = 0, \tag{3.8}$$

$$\tilde{\varphi}_{12r} - 2f_2 + \xi(\tilde{\varphi}_{13r} - 3f_3) = 0, \tag{3.9}$$

both evaluated at $r = 1$, where the subscripts r, θ represent differentiation with respect to those variables. If we eliminate $2f_2 + 3\xi f_3$ between (3.8) and (3.9), then the kinematic boundary condition becomes

$$\varphi_{11r} + \xi(\varphi_{12r} - \tilde{\varphi}_{12r}) + \xi^2\{\varphi_{13r} - \tilde{\varphi}_{13r} + \tfrac{1}{2}(\tilde{\varphi}_{12r}\varphi_{11rr} - \tilde{\varphi}_{12\theta r}\varphi_{11\theta})\} = 0 \quad \text{at } r = 1. \tag{3.10}$$

Substitution of (3.5), (3.6) into (2.5), and transfer of the boundary condition to $r = 1$ gives, for the pressure boundary condition,

$$\begin{aligned} &2(1-\alpha) + 2\tilde{\varphi}_{12} - \lambda^2(\varphi_{11r}^2 + \varphi_{11\theta}^2 + 2\varphi_{12}) \\ &\quad + \xi\{4\tilde{\varphi}_{13} - \lambda^2(2\varphi_{11r}\varphi_{12r} + 2\varphi_{11\theta}\varphi_{12\theta} + 4\varphi_{13})\} = 0 \quad \text{at } r = 1. \end{aligned} \tag{3.11}$$

We now determine explicitly the terms $O(\epsilon)$ shown in (3.5), (3.6) by substituting these expansions into (3.4) with (2.7), (3.10), (3.11) and equating to zero coefficients of successive powers of ξ.

The leading-order terms result in the following problem for φ_{11}:

$$\left.\begin{aligned} &\nabla^2\varphi_{11} = 0, \\ \text{with} \quad &\varphi_{11r} = 0 \quad \text{at } r = 1, \quad \varphi_{11} \sim \frac{r}{\lambda}\cos\theta \quad \text{as } r \to \infty. \end{aligned}\right\} \tag{3.12}$$

The solution for φ_{11}, already anticipated in (3.1), is

$$\varphi_{11} = \frac{1}{\lambda}\left(r + \frac{1}{r}\right)\cos\theta. \tag{3.13}$$

The terms $O(\xi)$ in (3.4), (3.10), and $O(1)$ in (3.11), now give, for $\varphi_{12}, \tilde{\varphi}_{12}$

$$\left.\begin{aligned} &\nabla^2\varphi_{12} = \nabla^2\tilde{\varphi}_{12} = 0, \\ \text{with, at } r = 1, \quad &\tilde{\varphi}_{12r} - \varphi_{12r} = 0, \\ &\tilde{\varphi}_{12} - \lambda^2\varphi_{12} = \alpha - \cos 2\theta, \end{aligned}\right\} \tag{3.14}$$

where use has been made of (3.13). If we write

$$\varphi_{12} = \sum_{n=1}^{\infty} a_n r^{-n} \cos n\theta, \quad \tilde{\varphi}_{12} = \sum_{n=0}^{\infty} \tilde{a}_n r^n \cos n\theta,$$

where due attention has been paid to conditions at infinity and $r = 0$, then it is readily shown, by substitution into (3.14), that $\tilde{a}_0 = \alpha$, $a_2 = -\tilde{a}_2 = (1+\lambda^2)^{-1}$, $a_n = \tilde{a}_n = 0$ otherwise, so that

$$\varphi_{12} = \frac{1}{1+\lambda^2}\frac{\cos 2\theta}{r^2}, \quad \tilde{\varphi}_{12} = \alpha - \frac{r^2}{1+\lambda^2}\cos 2\theta. \tag{3.15}$$

The solution at this order is completed by determining the jet shape function $f_2(\theta)$ which, from (3.9), is given by

$$f_2(\theta) = \tfrac{1}{2}\tilde{\varphi}_{12r}(r=1) = -\frac{1}{1+\lambda^2}\cos 2\theta. \tag{3.16}$$

Before we move to the next stage we make two observations. The first is that (3.16) implies a symmetric deformation of the jet cross-section from its original circular shape, and the second that an increase in pipe pressure ($\alpha > 0$) results in an acceleration of the emerging jet flow by (3.15).

We move next to the consideration of $\varphi_{13}, \tilde{\varphi}_{13}$ which, from (3.4)–(3.6), (3.10), (3.13) and (3.15) satisfy

$$\left.\begin{aligned} \nabla^2\varphi_{13} = \nabla^2\tilde{\varphi}_{13} = 0, \\ \text{together with, at } r = 1, \\ \tilde{\varphi}_{13r} - \varphi_{13r} = \frac{1}{\lambda(1+\lambda^2)}(\cos\theta - 3\cos 3\theta), \\ \tilde{\varphi}_{13} - \lambda^2\varphi_{13} = \frac{\lambda}{1+\lambda^2}(\cos\theta - \cos 3\theta). \end{aligned}\right\} \tag{3.17}$$

If we again express the solutions in the form

$$\varphi_{13} = \sum_{n=1}^{\infty} b_n r^{-n} \cos n\theta, \quad \tilde{\varphi}_{13} = \sum_{n=0}^{\infty} \tilde{b}_n r^n \cos n\theta,$$

then it is a straightforward matter to show that

$$\left.\begin{aligned} b_1 = -b_3 = \frac{1}{\lambda}\frac{1-\lambda^2}{(1+\lambda^2)^2}, \\ \tilde{b}_1 = -\tilde{b}_3 = \frac{2\lambda}{(1+\lambda^2)^2}, \end{aligned}\right\} \tag{3.18}$$

with all other $b_n, \tilde{b}_n \equiv 0$, to give

$$\varphi_{13} = \frac{1}{\lambda}\frac{1-\lambda^2}{(1+\lambda^2)^2}\left(\frac{\cos\theta}{r} - \frac{\cos 3\theta}{r^3}\right), \quad \tilde{\varphi}_{13} = \frac{2\lambda}{(1+\lambda^2)^2}(r\cos\theta - r^3\cos 3\theta).$$

The solution at this stage is completed by noting, from (3.9), that

$$f_3(\theta) = \tfrac{1}{3}\tilde{\varphi}_{13r}(r=1) = \frac{2}{3}\frac{\lambda}{(1+\lambda^2)^2}(\cos\theta - 3\cos 3\theta). \tag{3.19}$$

The jet shape function $f_3(\theta)$ in (3.19) shows an asymmetric distortion of the jet cross-

section. This asymmetry is associated with a corresponding asymmetry of the pressure distribution. The jet pressure $\tilde{p}$ is readily calculated from the inner solution, up to the point that we have taken it, as

$$\tilde{p}-p_{-\infty} = -\epsilon^2(\tilde{\varphi}_{12}+2\xi\tilde{\varphi}_{13}) = -\epsilon^2\left\{\alpha-\frac{r^2}{1+\lambda^2}\cos 2\theta+4\xi\frac{\lambda}{(1+\lambda^2)^2}(r\cos\theta-r^3\cos 3\theta)\right\}. \tag{3.20}$$

So far as the terms $O(\epsilon^3)$ in (3.5), (3.6) are concerned we simply note, by substitution into (3.4), that φ_{31} and $\tilde{\varphi}_{31}$ satisfy the equations

$$\nabla^2\varphi_{31}+2\varphi_{13} = \nabla^2\tilde{\varphi}_{31}+2\tilde{\varphi}_{13} = 0. \tag{3.21}$$

It is at this point that the solution would involve functions that are not solutions of the two-dimensional form of Laplace's equation.

The series (3.5), (3.6) are valid in the far field; they fail in the neighbourhood of $x = 0$ since no account is taken in them of the presence of the pipe orifice. Written in terms of the original variable x we have

$$\left.\begin{aligned}\varphi &\sim \lambda x+\epsilon\lambda\varphi_{11}+\epsilon^2\lambda x\varphi_{12}+\epsilon^3\lambda(x^2\varphi_{13}+\varphi_{31})+\ldots,\\ \tilde{\varphi} &\sim x+\epsilon^2 x\tilde{\varphi}_{12}+\epsilon^3(x^2\tilde{\varphi}_{13}+\tilde{\varphi}_{31})+\ldots.\end{aligned}\right\} \tag{3.22}$$

Note that the coefficient of each power of ϵ is a solution of (2.2), that of ϵ^3 by virtue of (3.21). The expressions (3.22) are the asymptotic forms that a solution, valid in the neighbourhood of the pipe orifice, must take as $x\to\infty$. We now consider such a solution.

3.2. *The near-field solution: $x = O(1)$*

Correct to $O(\epsilon^2)$ we write

$$\left.\begin{aligned}\varphi &= \lambda x+\epsilon\lambda\varphi_{11}(r,\theta)+\epsilon^2\psi(r,\theta,x),\\ \tilde{\varphi} &= x+\epsilon^2\tilde{\psi}(r,\theta,x).\end{aligned}\right\} \tag{3.23}$$

The unknowns $\psi, \tilde{\psi}$ each satisfy (2.2) together with

$$\nabla\psi \sim \mathbf{0} \quad \text{as } r\to\infty; \tag{3.24}$$

$$\nabla\psi, \nabla\tilde{\psi} \sim \mathbf{0} \quad \text{as } x\to-\infty; \tag{3.25}$$

and, as required by matching,

$$\psi \sim \frac{\lambda}{1+\lambda^2}\frac{x}{r^2}\cos 2\theta, \quad \tilde{\psi} \sim \alpha x-\frac{1}{1+\lambda^2}xr^2\cos 2\theta \quad \text{as } x\to\infty. \tag{3.26a,b}$$

The condition at the surface of the pipe gives

$$\frac{\partial\psi}{\partial r} = \frac{\partial\tilde{\psi}}{\partial r} = 0, \quad r = 1, \quad x < 0. \tag{3.27}$$

Finally the kinematic and dynamic boundary conditions at the jet surface require, respectively,

$$\left.\begin{aligned}\psi_r-\lambda\tilde{\psi}_r &= 0, &(3.28a)\\ \tilde{\psi}_x-\lambda\psi_x &= \alpha-\cos 2\theta, &(3.28b)\end{aligned}\right\} \quad \text{at } r = 1, \quad x > 0,$$

where at this order no additional terms arise from the transference of boundary conditions to $r = 1$.

It proves convenient to separate $\psi, \tilde{\psi}$ into symmetric and asymmetric parts. Thus we write

$$\psi = \psi_0 + \psi_2, \quad \tilde{\psi} = \tilde{\psi}_0 + \tilde{\psi}_2. \tag{3.29a}$$

We consider first the symmetric problem for $\psi_0, \tilde{\psi}_0$ and we note in particular, from (3.26*b*) and (3.28*b*),

$$\tilde{\psi}_0 \sim \alpha x \quad \text{as } x \to \infty; \quad \tilde{\psi}_{0x} - \lambda \psi_{0x} = \alpha \quad \text{at } r = 1, \quad x > 0. \tag{3.29b}$$

The potential problem for the outer and inner flows, with the conditions (3.24)–(3.28) has been solved by the Wiener–Hopf technique, the not inconsiderable details of which are presented in Appendix A. Here we summarize the main features of the solutions that have been obtained.

(i) $x \leqslant 0, \quad r \leqslant 1$

In this region we have, from (A 37),

$$\tilde{\psi}_0(r, x) = -\frac{\alpha}{\sqrt{2}} \sum_{n=1}^{\infty} \frac{J_0(\mu_n r)\, \mathrm{e}^{-\mu_n |x|}}{\mu_n^2 J_1'(\mu_n) K_+(\mathrm{i}\mu_n)}, \tag{3.30}$$

where the physically irrelevant constant C_1 has been omitted and the constants μ_n are the solutions of $J_1(\mu) = 0$, where J_1 is the Bessel function of order one. The function K_+ has not been evaluated explicitly but is determined through (A 23). One of the main features to note of the solution (3.30) is that the disturbance to the uniform flow within the pipe decays very rapidly with distance from the orifice. The decay is dominated by the factor $\mathrm{e}^{-\mu_1 |x|}$ where $\mu_1 \approx 3.86$.

(ii) $x \geqslant 0, \quad r \leqslant 1$

The perturbation potential within the jet is given by (A 38) as

$$\tilde{\psi}_0(r, x) = \alpha x + \frac{\alpha \lambda^2}{2^{\frac{3}{2}} \pi} \int_0^{\infty} \frac{K_-(-\mathrm{i}p) J_0(pr) \{K_0'(\mathrm{i}p) + K_0'(-\mathrm{i}p)\} \mathrm{e}^{-px}\, \mathrm{d}p}{\{\lambda^2 + (1-\lambda^2)\, \mathrm{i}p J_0(p) K_0'(-\mathrm{i}p)\} \{\lambda^2 - (1-\lambda^2)\, \mathrm{i}p J_0(p) K_0'(\mathrm{i}p)\}}, \tag{3.31}$$

where the function K_- may be determined through (A 23), and K_0 is a modified Bessel function of order zero. The behaviour of $\tilde{\psi}_0$ in (3.31) as $x \to \infty$ has been determined by an application of Laplace's method to give

$$\tilde{\psi}_0(r, x) \sim \alpha x \left(1 + \frac{\lambda^2}{4x^2}\right) \quad \text{as } x \to \infty. \tag{3.32}$$

(iii) $r \geqslant 1, \quad$ *all* x

For the region external to both the pipe and the jet we have, from (A 39),

$$\psi_0(r, x) = -\frac{\mathrm{i}\alpha\lambda}{2^{\frac{3}{2}} \pi} \int_{-\infty}^{\infty} \frac{K_0(|\sigma| r)\, \mathrm{e}^{-\mathrm{i}\sigma x}\, \mathrm{d}\sigma}{K_+(\sigma) K_0'(|\sigma|)\, \sigma |\sigma|}. \tag{3.33}$$

Again it is of interest to determine the far-field behaviour of ψ_0. This is accomplished by an application of the method of steepest descents which shows that

$$\psi_0(r, x) \sim \frac{\alpha\lambda}{4(r^2 + x^2)^{\frac{1}{2}}} \quad \text{as } |x|, r \to \infty. \tag{3.34}$$

It is interesting to note that whilst the disturbance engendered by the pipe orifice decays exponentially within the pipe, see (3.30), it decays only algebraically outside the pipe where it displays a source-like behaviour.

We consider next the asymmetric part of (3.29) namely ψ_2 and $\tilde{\psi}_2$. We note in particular from (3.26) and (3.28*b*) that

$$\left.\begin{aligned} &\psi_2 \sim \frac{\lambda}{1+\lambda^2}\frac{x}{r^2}\cos 2\theta, \quad \tilde{\psi}_2 \sim -\frac{1}{1+\lambda^2} x r^2 \cos 2\theta \quad \text{as } x \to \infty \\ \text{and} \quad &\tilde{\psi}_{2x} - \lambda \psi_{2x} = -\cos 2\theta \quad \text{at } r = 1, \quad x > 0. \end{aligned}\right\} \tag{3.35}$$

The details of the method of solution for $\psi_2, \tilde{\psi}_2$ are given in Appendix B, here we summarize the main features of the solution.

(iv) $x \leqslant 0, \quad r \leqslant 1$

In this region we have, from (B 22*a*),

$$\tilde{\psi}_2(r,\theta,x) = \frac{\sqrt{2}\cos 2\theta}{(1+\lambda^2)^{\frac{1}{2}}} \sum_{n=1}^{\infty} (1+A\Omega_n) \frac{J_2(\Omega_n r)\, \mathrm{e}^{-\Omega_n |x|}}{\Omega_n^3 \bar{K}_+(\mathrm{i}\Omega_n) J_2''(\Omega_n)}, \tag{3.36}$$

where $\bar{K}_+$ may be inferred from (B 15), A is a constant defined Appendix B and the Ω_n are the positive zeros of $J_2'(\Omega)$, where J_2 is the Bessel function of order two. As $x \to -\infty$ in the pipe we see from (3.36) that

$$\tilde{\psi}_2(r,\theta,x) \sim \frac{\sqrt{2}(1+A\Omega_1) J_2(\Omega_1 r)\, \mathrm{e}^{-\Omega_1 |x|} \cos 2\theta}{(1+\lambda^2)^{\frac{1}{2}} \Omega_1^3 \bar{K}_+(\mathrm{i}\Omega_1) J_2''(\Omega_1)}, \quad x \to -\infty, \tag{3.37}$$

where $\Omega_1 \approx 3.05$. Again we note a very rapid decay of the disturbance in the pipe.

(v) $x \geqslant 0, \quad r \leqslant 1$

In this jet region the perturbation potential may be written, see (B 22*b*), as

$$\tilde{\psi}_2(r,\theta,x) = -\frac{x r^2 \cos 2\theta}{1+\lambda^2} - \frac{\mathrm{i}\cos 2\theta}{\sqrt{2\pi}(1+\lambda^2)^{\frac{1}{2}}} \int_0^{\infty} \hat{K}(p) \frac{J_2(pr)\, \bar{K}_-(-\mathrm{i}p)}{p^2} \mathrm{e}^{-px} (1+Ap)\, \mathrm{d}p, \tag{3.38}$$

where $\hat{K}(p)$ is defined in (B 19), and $\bar{K}_-$ may be inferred through (B 15). For large x the integral in (3.38) may again be estimated using Laplace's method to give

$$\tilde{\psi}_2(r,\theta,x) \sim -\frac{x r^2 \cos 2\theta}{1+\lambda^2}\left\{1 - \frac{\lambda^2}{8(1+\lambda^2)x^4}\right\} \quad \text{as } x \to \infty. \tag{3.39}$$

(vi) $x \leqslant 0, \quad r \geqslant 1$

Outside the pipe, in $x < 0$, we have from (B 23*a*)

$$\psi_2(r,\theta,x) = -\frac{\lambda \cos 2\theta}{\sqrt{2\pi}(1+\lambda^2)^{\frac{1}{2}}} \int_0^{\infty} \left\{\frac{K_2(\mathrm{i}pr)}{K_2'(\mathrm{i}p)} + \frac{K_2(-\mathrm{i}pr)}{K_2'(-\mathrm{i}p)}\right\} \frac{\mathrm{e}^{-p|x|}}{p^3 \bar{K}_+(\mathrm{i}p)} (1+Ap)\, \mathrm{d}p, \tag{3.40}$$

where K_2 is a modified Bessel function of the second order. From (3.40) we may infer, again using Laplace's method, that for fixed r, and as $x \to -\infty$,

$$\psi_2(r,\theta,x) \sim -\frac{\lambda(r^4+1)\cos 2\theta}{16 r^2 x^2 (1+\lambda^2)} \quad \text{as } x \to -\infty. \tag{3.41}$$

(vii) $x \geqslant 0, \quad r \geqslant 1$

Finally, outside the jet in $x > 0$ the perturbation potential is given by, see (B 23b),

$$\psi_2(r,\theta,x) = \frac{\lambda x\cos 2\theta}{(1+\lambda^2)r^2} - \frac{\lambda\cos 2\theta}{\sqrt{2\pi}(1+\lambda^2)^{\frac{1}{2}}}\int_0^\infty \left\{\frac{\mathrm{i}K_2(\mathrm{i}pr)}{I_2(\mathrm{i}p)K_2'(\mathrm{i}p)-\lambda^2K_2(\mathrm{i}p)I_2'(\mathrm{i}p)}\right.$$
$$\left. + \frac{\mathrm{i}K_2(-\mathrm{i}pr)}{I_2(\mathrm{i}p)K_2'(-\mathrm{i}p)+\lambda^2K_2(-\mathrm{i}p)I_2'(\mathrm{i}p)}\right\}\frac{\bar{K}_-(-\mathrm{i}p)I_2'(\mathrm{i}p)\,\mathrm{e}^{-px}}{p^2}(1-Ap)\,\mathrm{d}p, \tag{3.42}$$

where I_2 is a modified Bessel function of the second kind. The far-field, asymptotic form of (3.42), valid as $x\to\infty$ with r fixed, is obtained by Laplace's method as

$$\psi_2(r,\theta,x) \sim \frac{\lambda x\cos 2\theta}{(1+\lambda^2)r^2}\left\{1+\frac{(1-\lambda^2)(1+\lambda^2)^{-1}+r^4}{16x^4}\right\} \quad \text{as } x\to\infty. \tag{3.43}$$

This completes the discussion of the near-field solution which describes the interaction in the neighbourhood of the pipe orifice.

3.3. *Jet force and displacement*

Before leaving this section we employ the far-field solution of §3.1 to calculate the force on, and displacement of, the jet.

In the crossflow direction the force acting, per unit length of the jet, is to lowest order

$$\bar{F} = -\rho U_0^2 a\int_0^{2\pi} p_s\cos\theta\,\mathrm{d}\theta = \frac{4\pi a\rho U_0^2\epsilon^2\lambda}{(1+\lambda^2)^2}\xi,$$

using the expression for $p_s = \tilde{p}|_{r=1}$ given from (3.20). A suitably defined force coefficient C_F is then

$$C_F = \frac{\bar{F}}{\frac{1}{2}\rho(\epsilon U_0)^2 2a} = 4\pi\beta\frac{\lambda^2 x}{(1+\lambda^2)^2} \leqslant \pi\beta x, \tag{3.44}$$

where $\beta = \epsilon/\lambda$, and is the inclination of the jet pipe to the undisturbed outer stream direction when this is small.

Associated with this force is a displacement of the jet that we estimate as follows. If we write the jet surface as $r = 1+f(\xi,\theta)$, where f may be inferred from (3.7), then the area A of the jet cross-section is given by

$$A = 2\int_0^\pi\int_0^{1+f} r\,\mathrm{d}r\,\mathrm{d}\theta = \pi + O(\xi^4).$$

We define the moment of this area as

$$hA = 2\int_0^\pi\int_0^{1+f} r^2\cos\theta\,\mathrm{d}r\,\mathrm{d}\theta = \frac{2}{3}\frac{\pi\lambda}{(1+\lambda^2)^2}\xi^3 + O(\xi^5),$$

from which we infer that the displacement of the jet centroid is given by

$$h = \frac{2}{3}\frac{\lambda}{(1+\lambda^2)^2}\xi^3 + O(\xi^5). \tag{3.45}$$

4. Discussion

The dominant features of the solution obtained are easily explained in qualitative terms. The crossflow around the nearly circular jet induces low pressures on the sides of the jet and high pressures fore and aft. The jet contour responds by expanding

laterally and contracting in the fore-and-aft direction, preserving its area, by continuity. This corresponds to the approximately elliptic form of the jet cross-section at leading order, as given by (3.16) in (3.7). The pressure within the jet adapts, with an increase in axial speed along the sides and a reduction fore and aft, as given by (3.15) in (3.6). In the absence of a component of the ambient flow parallel to the axis of the pipe, $\lambda = 0$, the next terms in the surface pressure (3.20) and jet shape (3.19) vanish. In the presence of an axial flow, with $\lambda > 0$, we can regard the jet as a solid body at an angle of incidence to a uniform stream, and apply the ideas of slender-body theory. The growth in the lateral dimension or 'span' of the elliptic cross-section gives a 'lift' force in the direction of the crossflow. The associated surface pressure distribution has suction peaks towards the lateral extremities of the leeward face of the jet, and these peaks draw out the surface into lobes, as given by (3.19) and illustrated in figure 2. To recover the correct force, as given by (3.44), from slender-body theory, this further deformation must be represented.

The transverse 'lift' force acting on the jet produces the centripetal acceleration of the fluid inside the jet required to deflect it towards the direction of the ambient flow. Working for the moment in dimensional quantities for clarity, we have from (3.44) and (3.45):

for the force per unit length of the jet	$4\pi a\rho U_0^2 \lambda\epsilon^2\xi/(1+\lambda^2)^2$
for the mass per unit length of the jet	$\pi a^2\rho$
for the curvature of the jet centreline	$4\lambda\epsilon^2\xi/a(1+\lambda^2)^2$;

and so the elementary centripetal acceleration relation is recovered.

Having established the consistency of the major features of the solution, we turn to a more detailed discussion, considering first the role of the parameter α. To obtain an indication of this role, we first look at the axisymmetric jet given by allowing ϵ to tend to zero and α to tend simultaneously to infinity in such a way that $\bar{\alpha} = \alpha\epsilon^2$ remains finite and small compared with unity. The jet shape is then still a small perturbation of the circular cylinder defined by the pipe. Writing (2.1) in non-dimensional form gives, in this limit,

$$p_{-\infty} - p_\infty = \bar{\alpha}. \tag{4.1}$$

Away from the immediate neighbourhood of the orifice, the only disturbance remaining comes from $\tilde{\varphi}_{12}$ and expresses the fact that the non-dimensional jet speed is greater by $\bar{\alpha}$ than the speed in the pipe. As a result, the non-dimensional pressure in the jet is less by $\bar{\alpha}$ than the pressure $p_{-\infty}$ upstream in the pipe and therefore, by (4.1), equal to the ambient pressure. These changes in speed and pressure, and the associated change in diameter required by continuity, take place on the lengthscale of the pipe diameter, and are given in detail by (3.30)–(3.34). We note in passing that this behaviour depends on the magnitude λ of the coflow, except inside the pipe. However, the eventual effect is the equalization of the pressures in the inner and outer flows. It is, in fact, hard to imagine physical circumstances in which this equalization would not be accomplished inside the pipe, so that the appropriate value of $\bar{\alpha}$ would be zero. The presence of crossflow complicates the situation, but the following argument leads to the same conclusion. If we take the average of the pressure in the jet away from the neighbourhood of the orifice, as given by (3.20), we find $p_{-\infty} - \tilde{p}_{\text{mean}} = \alpha\epsilon^2$. Therefore, once the pressure in the jet has adjusted to ambient conditions, its mean level is lower by $\alpha\epsilon^2$ than the level upstream in the pipe. Again, it seems likely that this pressure adjustment would propagate up the pipe in most physical situations, so that $\alpha = 0$ would be the appropriate value.

Now we consider the behaviour at the orifice lip, where some form of Kutta condition should be satisfied. However, the behaviour of the solution quoted at the end of each Appendix indicates that the slope of the jet surface tends to infinity as the lip is approached. This result is inconsistent with the initial transfer of the boundary conditions to the cylindrical surface, and it indicates a non-uniformity in the near-field expansions. Further analysis suggests that this non-uniformity arises on a lengthscale of $a\epsilon^4$, and that it can be removed by solving a local problem which is two-dimensional but nonlinear. It is hoped to address this problem in a subsequent paper.

Setting this difficulty aside, we turn to a discussion of the effects of the parameter λ, for the case $\alpha = 0$. We have already remarked that, in the absence of a coflow, $\lambda = 0$, there is no force on the jet and no deflection of its centreline, to the order calculated. The disturbance velocity field near the orifice is always symmetric fore-and-aft to the order calculated, since the angular coordinate enters (3.36)–(3.43) as a factor $\cos 2\theta$. For $\lambda = 0$, the terms given so far show the shape is symmetric fore and aft on the larger scale also. Moreover, the simplification introduced by setting $\lambda = 0$ makes it practicable to calculate a further term in the expansion (3.7) for the jet shape, namely

$$f_4(\theta) = \tfrac{1}{4} - \tfrac{1}{3}\cos 2\theta + \tfrac{7}{12}\cos 4\theta. \tag{4.2}$$

The jet shape therefore remains symmetric fore and aft beyond the initial elliptic deformation. A further simplification is that the disturbance field outside the jet and pipe in the immediate neighbourhood of the orifice vanishes, to order ϵ^2, when $\lambda = 0$, as shown in (3.33), (3.40) and (3.42). This is consistent, in that the disturbance inside the jet is $O(\epsilon^2)$, so the shape change will be $O(\epsilon^2)$; this shape change in a coflow of speed λ gives a disturbance proportional to $\lambda\epsilon^2$, but in the crossflow of speed ϵ the disturbance is $O(\epsilon^3)$.

On the other hand, the disturbance field inside the pipe, given by (3.30) and (3.36) exhibits rapid exponential decay regardless of the value of λ. This suggests that a similar behaviour may be expected when a cylindrical jet exhausts through a circular orifice in an infinite plane.

When $\lambda > 0$ it is meaningful to write $\epsilon = \beta\lambda$, as in §3.3, so that the pipe is inclined at an angle $\tan^{-1}\beta$ to the ambient flow. The treatment is valid both for λ of order ϵ and β of order unity and for λ of order unity and β small, in which case β is the inclination of the pipe to the flow. In the former case, in which the ambient speed is small compared with the jet speed, it is consistent to neglect λ^2 compared with unity, thereby simplifying the formulae considerably. For example, both the force per unit length of the jet and the jet deflection, at a fixed distance x from the orifice, become proportional to $\lambda\epsilon^3$, according to §3.3. Hence if $\lambda^2+\epsilon^2$ is given, corresponding to a specified ambient speed, the maximum force and deflection arise when $\epsilon^2 = 3\lambda^2$, i.e. the pipe is inclined at 60° to the ambient velocity vector. On the other hand, if the coflow is comparable with the jet speed, so that $\beta \ll 1$, the inclination of the pipe will be small and approximately equal to β, and the force and deflection increase like β^3 for a given ambient speed λ. A numerical example calculated for $\lambda = 0.5$, $\epsilon = 0.1$ is shown in figures 2 and 3. Figure 2 shows the cross-sectional shapes of the jet, as given by (3.7), (3.16) and (3.19), for distances 1, 3, 5 and 7 pipe radii downstream of the orifice. At $x = 1$, the section is almost circular, at $x = 3$ it is approximately elliptic, at $x = 5$ it is kidney shaped, and at $x = 7$ it has taken on a lobed form. By $x = 7$, the assumption of an approximately circular cross-section is clearly inadequate

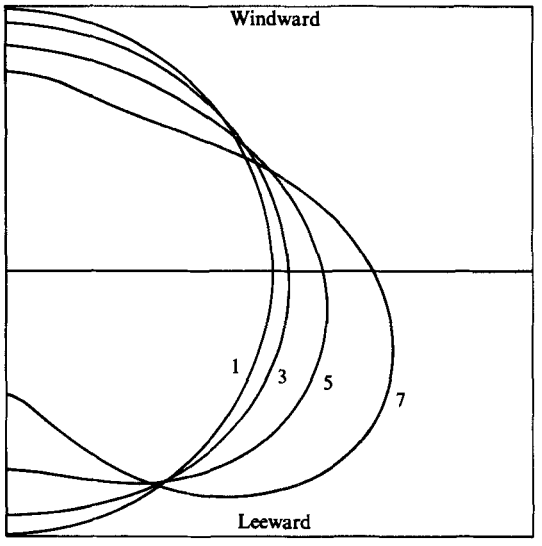

FIGURE 2. Cross-sectional shapes of the jet at $x = 1, 3, 5, 7$ for $\lambda = 0.5$, $\epsilon = 0.1$.

and it is unlikely that the present approach would be even qualitatively reliable further from the orifice. The results illustrate the difficulty of defining jet deflection in a realistic way. At $x = 7$, (3.45) shows that the centroid is deflected 0.073 radii downstream, but the mean position of the jet boundary in the plane of symmetry is just twice as far upstream, and the 'centre of the lobe' is judged by eye to be about twice as far again downstream.

In figure 3 are shown the corresponding distributions of non-dimensional pressure on the jet boundary, as given by (3.20). These are plotted round the circumference of the undeflected jet and normal to its circular boundary. The interaction between the shape and the pressure distribution is easily visualized. The surface pressure in the plane of symmetry is independent of x and given by

$$p - p_\infty = \frac{\frac{1}{2}\epsilon^2(1-\lambda^2)}{1+\lambda^2}. \tag{4.3}$$

This may be compared with the level upstream on the pipe in the same plane, corresponding to stagnation of the crossflow:

$$p - p_\infty = \tfrac{1}{2}\epsilon^2.$$

Thus we see that the pressure falls by $\lambda^2\epsilon^2/(1+\lambda^2)$ in the plane of symmetry near the orifice.

If $\lambda = 1$, so that the velocity of the coflow is equal to that in the pipe, we have a special case. In the absence of crossflow, there would be no jet. With crossflow, a vortex sheet remains and the solution resembles the vortex wake of an annular wing of vanishingly small aspect ratio. In particular, $\varphi_{13} \equiv 0$, by (3.18), and, by (4.3), the pressure on the jet in the plane of symmetry is the same as the undisturbed pressure of the ambient flow. The bound vortex lines in the pipe lie along its generators, but a glance at (3.16) shows that the 'trailing' vortex sheet contains a circumferential component as well.

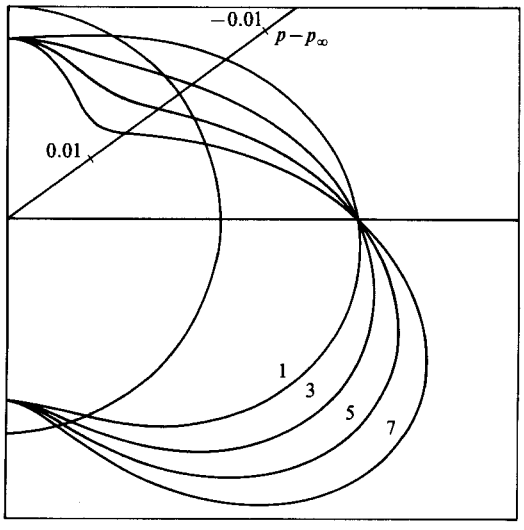

FIGURE 3. Jet surface pressure, plotted normal to the section of the undisturbed jet at $x = 1, 3, 5, 7$ for $\lambda = 0.5$, $\epsilon = 0.1$.

The behaviour of the vortex lines, defined as curves of constant $\varphi - \tilde{\varphi}$, for the more general case with $\lambda = 0.5$, $\epsilon = 0.1$ illustrated previously is shown in figure 4. The vortex lines are drawn on the surface of the undeflected jet, half of which is then unwrapped into the plane of the paper. Superimposed on the vortex lines are the mean streamlines, i.e. the streamlines of the mean of the surface velocity fields inside and outside. Since there is a difference of total pressure across the sheet, the vortex lines and mean streamlines are different. We note that the vortex lines become more closely aligned with the jet axis as the distance from the orifice increases, and that they lie closer together. This represents the formation of the vortices aligned with the jet axis which are a feature of the development of the jet in crossflow.

When $\lambda > 1$, the flow resembles a wake rather than a jet, with lower axial velocities inside than out. For a given pipe inclination β, both the force and the deflection at a given distance from the orifice are proportional to $\lambda^4/(1+\lambda^2)^2$, from (3.44) and (3.45). Both therefore increase monotonically with λ, as the jet or wake offers less resistance to the ambient flow. However, to maintain the assumptions of the treatment, β must become smaller as λ increases. By supposing $U_0 \to 0$ as $\lambda \to \infty$, keeping λU_0 fixed, with $\beta \to 0$, we find the solution corresponds to a uniform flow of speed λU_0 surrounding fluid at rest within an infinite circular cylinder.

So far we have assumed $\lambda \geqslant 0$. If a negative value of λ is introduced, the jet is apparently deflected upstream. It may be that a local behaviour of this kind is possible, but we must reject the idea of a jet penetrating to infinity against the crossflow. Although the problem has been formulated as a pair of potential problems, the matching condition requires the formation of a vortex sheet. Consequently, the allowable solutions must be at least weak solutions of the Euler equations governing inviscid rotational flow. For these equations, the streamlines are characteristics for the propagation of vorticity, so that in a properly posed problem vorticity must be specified upstream, or originate at a solid surface, and emerge downstream. It is of some interest to see how the derivation of the force on the jet from slender-body

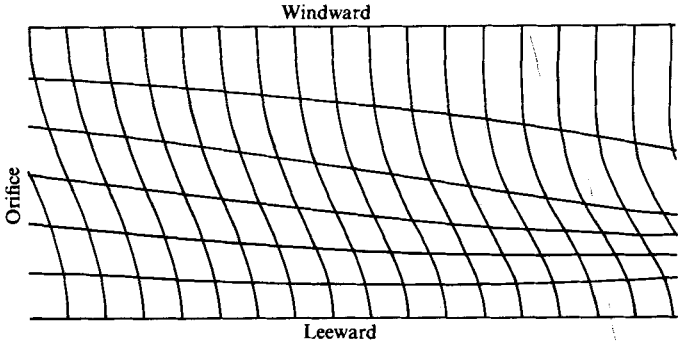

FIGURE 4. Vortex lines and mean streamlines in one half of the unwrapped surface of the jet for $\lambda = 0.5$, $\epsilon = 0.1$, $0 \leqslant x \leqslant 7$, $0 \leqslant \theta \leqslant \pi$. In this figure the scales are equal.

theory fares for a jet directed against the coflow. The jet now corresponds to a body at incidence with approximately elliptic cross-sections and with span decreasing in the direction of flow. In the absence of separation, the local lift is then negative, as the present treatment suggests. However, the overall force on the body, regarded as terminating in a circular base at the jet orifice, is positive. Once again then, an inconsistency arises if we try to extend the local solution to a global one.

Finally, we must return to our initial question: how far can the behaviour of the jet in crossflow be explained in inviscid terms? We have shown that, if the jet is initially directed downstream in the ambient flow, inviscid mechanisms produce a jet deflection, a jet distortion, and an axial vorticity increase qualitatively similar to those observed. In view of the central assumption that the jet remains close to a circular cylinder, it is clearly impossible to carry the present treatment far enough to warrant making quantitative comparisons. If the jet is initially directed upstream, no meaningful conclusion can be drawn from the present treatment. If the jet emerges exactly normal to the ambient flow, the present treatment predicts a growing distortion which eventually violates its assumptions, but no deflection. On the other hand, it does suggest that if a small downstream deflection should arise, inviscid mechanisms would increase it. The next step appears to be the application of a panel, or boundary-integral method, to seek a self-consistent global solution of the inviscid flow problem.

This work has been carried out with the support of the Procurement Executive, Ministry of Defence. The authors are grateful for useful discussions with Professor D. W. Moore and Dr C. C. Lytton.

Appendix A

In this Appendix we outline the solution of the problem for $\psi_0(r,x)$, $\tilde{\psi}_0(r,x)$ introduced in (3.29*a*). Both ψ_0 and $\tilde{\psi}_0$ are harmonic functions which satisfy the boundary conditions set out in (3.24), (3.25), (3.27), (3.28*a*) and (3.29*b*).

It is first convenient to introduce new dependent variables

$$\hat{\Phi}_0(r,x) = \tilde{\psi}_0(r,x) - \alpha x, \quad r < 1; \quad \Psi_0(r,x) = \psi_0(r,x), \quad r > 1. \qquad (\text{A } 1a,b)$$

Both $\hat{\Phi}_0$ and Ψ_0 are harmonic functions which, from (3.24)–(3.27) and (3.29*b*), satisfy

$$\nabla\hat{\Phi}_0 \to -\alpha i \quad \text{as } x \to -\infty, \quad \hat{\Phi}_0 \to 0 \quad \text{as } x \to \infty \quad \text{for } r < 1, \tag{A 2a,b}$$

$$\Psi_0 \to 0 \quad \text{as } |x|, r \to \infty \quad \text{for } r > 1, \tag{A 2c}$$

together with, at $r = 1$,

$$\frac{\partial\Psi_0}{\partial r} = \frac{\partial\hat{\Phi}_0}{\partial r} = 0 \quad \text{in } x < 0; \quad \frac{\partial\Psi_0}{\partial r} = \lambda\frac{\partial\hat{\Phi}_0}{\partial r}, \quad \lambda\frac{\partial\Psi_0}{\partial x} = \frac{\partial\hat{\Phi}_0}{\partial x} \quad \text{in } x > 0. \tag{A 2d,e,f,g}$$

In order to exploit the Wiener–Hopf technique the strategy that we now adopt is to solve, not a harmonic problem with conditions (A 2), but a Helmholtz problem in which $\hat{\Phi}_0$ and Ψ_0 satisfy

$$\Delta^2\hat{\Phi}_0 - \delta^2\Phi_0 = 0, \quad r < 1; \quad \Delta^2\Psi_0 - \delta^2\Psi_0 = 0, \quad r > 1, \tag{A 3a,b}$$

where δ is a constant such that $0 < \delta \ll 1$ and $\Delta^2 = \nabla^2 + \partial^2/\partial x^2$ is the three-dimensional Laplace operator. The equations (A 3) are to be solved subject to the conditions (A 2), but with the far-field condition (A 2*a*) replaced by $\hat{\Phi}_0 \sim a\,\mathrm{e}^{-\delta x}$ as $x \to -\infty$, where a is a constant, to be chosen such that in the limit $\delta \to 0$ the solution of the Helmholtz problem reduces to that of the original harmonic problem. Now, it can be shown that the far-field behaviour of $\hat{\Phi}_0$ and Ψ_0 gives

$$\left.\begin{aligned} \hat{\Phi}_0(r,x) &\sim \begin{cases} a(\mathrm{e}^{-\delta x} + a_1\,\mathrm{e}^{\delta x}) & \text{as } x \to -\infty \\ b_1\,\mathrm{e}^{-\delta x}/x & \text{as } x \to \infty \end{cases} \\ \Psi_0(r,x) &\sim c_1\,\mathrm{e}^{-\delta\hat{R}}/\hat{R} \qquad \text{as } \hat{R} \to \infty, \end{aligned}\right\} \tag{A 4}$$

where a_1, b_1 and c_1 are constants, and $\hat{R}^2 = r^2 + x^2$. To remove the exponentially growing part of $\hat{\Phi}_0$ as $x \to -\infty$ we introduce Φ_0 such that

$$\Phi_0(r,x) = \hat{\Phi}_0(r,x) - a\,\mathrm{e}^{-\delta x}, \tag{A 5a}$$

with

$$\Delta^2\Phi_0 - \delta^2\Phi_0 = 0, \tag{A 5b}$$

and

$$\frac{\partial\Phi_0}{\partial r} = 0 \quad \text{on } r = 1, \quad x < 0, \tag{A 5c}$$

$$\lambda\frac{\partial\Phi_0}{\partial r} = \frac{\partial\Psi_0}{\partial r}, \quad \frac{\partial\Phi_0}{\partial x} = \lambda\frac{\partial\Psi_0}{\partial x} + a\delta\,\mathrm{e}^{-\delta x} \quad \text{on } r = 1, \quad x > 0. \tag{A 5d,e}$$

We note that it may now be shown that

$$|\Phi_0| \sim \bar{A}\,\mathrm{e}^{-\delta|x|}, \quad |\Psi_0| \sim \bar{B}\,\mathrm{e}^{-\delta|x|} \quad \text{as } |x| \to \infty \tag{A 6}$$

for some constants $\bar{A}$ and $\bar{B}$. The problem posed for $\Phi_0(r,x)$ and $\Psi_0(r,x)$ in the foregoing is a Wiener–Hopf problem. To solve this we first define the Fourier transform of Φ_0 as

$$\bar{\varphi}(s,r) = \int_{-\infty}^{\infty} \Phi_0(r,x)\,\mathrm{e}^{\mathrm{i}sx}\,\mathrm{d}x, \tag{A 7}$$

with a similar expression for the transform $\bar{\psi}$ of Ψ_0. In (A 7) $s = \sigma + \mathrm{i}\tau$ is a complex variable, and it can be shown from the condition (A 6) that both $\bar{\psi}$ and $\bar{\varphi}$ are analytic

functions of s in the strip $R = \{s: -\delta < \tau < \delta\}$. We also define the half-range Fourier transforms

$$\bar{\varphi}_+(s,r) = \int_0^\infty \boldsymbol{\Phi}_0(r,x)\, e^{isx}\, dx, \quad \bar{\varphi}_-(s,r) = \int_{-\infty}^0 \boldsymbol{\Phi}_0(r,x)\, e^{isx}\, dx, \qquad (A\ 8a,b)$$

with similar expressions for $\bar{\psi}_+(r,x)$ and $\bar{\psi}_-(r,x)$, the half-range transforms of $\boldsymbol{\Psi}_0(r,x)$. We may deduce, upon using (A 6), that $\bar{\varphi}_+$ and $\bar{\psi}_+$ are analytic in the region $R_+ = \{s: \tau > -\delta\}$, whilst $\bar{\varphi}_-$ and $\bar{\psi}_-$ are analytic in $R_- = \{s: \tau < \delta\}$. To ensure that $\boldsymbol{\Phi}_0$ and $\boldsymbol{\Psi}_0$ have, at worst, an integrable singularity as $x \to \pm 0$ we also require $\bar{\varphi}_+$, $\bar{\psi}_+$, $\bar{\varphi}_-$ and $\bar{\psi}_-$ to decay algebraically as $|s| \to \infty$, in R_+ and R_- respectively. We note the relations

$$\bar{\varphi}(s,r) = \bar{\varphi}_+(s,r) + \bar{\varphi}_-(s,r), \quad \bar{\psi}(s,r) = \bar{\psi}_+(s,r) + \bar{\psi}_-(s,r); \quad s \in R. \qquad (A\ 9a,b)$$

Consider now the solution of (A 3b) that is appropriate to the region $r > 1$. The full-range transform of (A 3b) gives

$$\frac{1}{r}\frac{\partial}{\partial r}\left(r\frac{\partial \bar{\psi}}{\partial r}\right) - \gamma^2(s)\,\bar{\psi} = 0; \quad s \in R, \qquad (A\ 10)$$

where

$$\gamma(s) = (s + i\delta)^{\frac{1}{2}}(s - i\delta)^{\frac{1}{2}}. \qquad (A\ 11)$$

We make $\gamma(s)$ single-valued by introducing branch cuts at $s = \pm i\delta$; these are chosen to lie on the imaginary axis outside the region R. We choose the branch of $\gamma(s)$ that is real and positive on the real s-axis from which it follows that $\mathrm{Re}\,(\gamma) > 0$ in the entire cut plane. With $\gamma(s)$ so defined the solution of (A 10) that remains bounded in R as $r \to \infty$ is

$$\bar{\psi}(s,r) = A(s)\, K_0(\gamma r); \quad s \in R, \qquad (A\ 12)$$

where K_0 is a modified Bessel function of order zero, and $A(s)$ an, as yet, unknown function. Before we consider the boundary conditions at $r = 1$ we introduce the notation $\varphi_+ = \bar{\varphi}_+(s,1)$, $\varphi'_+ = \partial\bar{\varphi}_+(s,1)/\partial r$, etc. The half-range transforms of conditions (A 2d) and (A 5c,d,e) give

$$\varphi'_- = \psi'_- = 0; \qquad s \in R_-, \qquad (A\ 13a,b)$$

$$\psi'_+ - \lambda\varphi'_+ = 0; \qquad s \in R_+, \qquad (A\ 13c)$$

$$\lambda\psi_+ - \varphi_+ = \frac{i\{\lambda\boldsymbol{\Psi}_0(1,0) - \boldsymbol{\Phi}_0(1,0)\}}{s} + \frac{a\delta}{s(s+i\delta)}; \quad s \in R_+. \qquad (A\ 13d)$$

Since ψ_+ and φ_+ must both be analytic in R_+ we must remove the pole at $s = 0$ by choosing $\lambda\boldsymbol{\Psi}_0(1,0) - \boldsymbol{\Phi}_0(1,0) = a$ so that (A 13d) becomes

$$\lambda\psi_+ - \varphi_+ = \frac{ia}{s+i\delta}; \quad s \in R_+. \qquad (A\ 13e)$$

Also, eliminating $A(s)$ from (A 12), and using (A 9b), we have

$$\psi_+ + \psi_- = \frac{K_0(\gamma)}{\gamma K'_0(\gamma)}(\psi'_+ + \psi'_-); \quad s \in R. \qquad (A\ 13f)$$

We now consider the solution in $r < 1$. The appropriate solution of the full-range transform of (A 5b) in $r < 1$ is given by

$$\bar{\varphi}(s,r) = B(s)\, I_0(\gamma r); \quad s \in R, \qquad (A\ 14)$$

where I_0 is a modified Bessel function. From (A 15) and its derivative evaluated on $r = 1$ we have, when $B(s)$ is eliminated, and use is made of (A 9a),

$$\varphi_+ + \varphi_- = \frac{I_0(\gamma)}{\gamma I_0'(\gamma)}(\varphi_+' + \varphi_-'); \quad s \in R. \tag{A 15}$$

(A 15) with (A 13) now provides us with a total of six relationships between the eight unknowns $\varphi_\pm, \varphi_\pm', \psi_\pm, \psi_\pm'$. The analyticity properties that are required of these unknown functions make the system determinate provided that (A 13) and (A 15) can be rearranged to obtain a Wiener–Hopf equation.

To proceed, we first eliminate ψ_+, ψ_+', ψ_-' and φ_-' from (A 13f) and (A 15), making use of (A 13a–c, e) to give

$$\varphi_+ + \lambda\psi_- + \frac{\mathrm{i}a}{s+\mathrm{i}\delta} = \frac{\lambda^2 K_0(\gamma)}{\gamma K_0'(\gamma)}\varphi_+'; \quad s \in R, \quad \varphi_+ + \varphi_- = \frac{I_0(\gamma)}{\gamma I_0'(\gamma)}\varphi_+'; \quad s \in R. \tag{A 16a, b}$$

If we now subtract (A 16a) from (A 16b) we find, after some manipulation,

$$K(s)\,\eta_+(s) + \eta_-(s) = -\frac{\mathrm{i}a}{s+\mathrm{i}\delta}; \quad s \in R, \tag{A 17}$$

where $$\eta_+ \equiv \varphi_+', \quad \eta_- \equiv \lambda\psi_- - \varphi_-, \quad K(s) = \frac{\{(1-\lambda^2)\gamma I_0(\gamma) K_0'(\gamma) - \lambda^2\}}{\gamma^2 K_0'(\gamma) I_0'(\gamma)}. \tag{A 18a, b, c}$$

It can be shown that $K(s)$ is analytic in R and, with the constant λ not far from unity, an application of Rouché's theorem shows that K is non-zero in the entire cut plane. With these properties for $K(s)$, (A 17) is a Wiener–Hopf equation for η_+ and η_- defined in the strip R.

Consider the kernel $K(s)$ in (A 17), which is defined in (A 18c). It is readily shown that K is an even function in the cut plane and that

$$K(s) \sim \frac{(1+\lambda^2)}{\gamma(s)} \quad \text{as } |s| \to \infty. \tag{A 19}$$

Our aim now is to find functions $K_+(s)$ and $K_-(s)$ which are, respectively, analytic and non-zero in R_+ and R_- such that

$$K(s) = K_+(s)\,K_-(s), \tag{A 20}$$

for each s in R. To accomplish this we first write

$$F(s) = \log\frac{\gamma(s)\,K(s)}{1+\lambda^2} = F_+(s) + F_-(s); \quad s \in R, \tag{A 21}$$

where the branch of the logarithm in (A 21) is chosen such that $F(s) \to 0$ as $\mathrm{Re}\,(s) \to \infty$ in R, which also ensures that $F(s) \to 0$ as $\mathrm{Re}\,(s) \to -\infty$ in R since $\gamma(s)\,K(s)$ is an even function of s in R. The Cauchy integrals can be used to define $F_+(s)$, $F_-(s)$ as

$$F_\pm(s) = \pm\frac{1}{2\pi\mathrm{i}}\int_{C_\pm}\frac{F(\xi)}{\xi - s}\mathrm{d}\xi; \quad s \in R_\pm, \tag{A 22}$$

where C_+, C_- are contours which each run from $\xi = -\infty$ to $\xi = +\infty$ in R; C_+ passes below the point $\xi = s$ whilst C_- passes above that point. It may be shown that F_+ and

F_- are analytic in R_+ and R_- respectively, and in terms of them the functions K_+ and K_- in (A 20) are given by

$$\left.\begin{aligned} K_+(s) &= \frac{(1+\lambda^2)^{\frac{1}{2}} \exp\{F_+(s)+\tfrac{1}{4}\pi i\}}{(s+i\delta)^{\frac{1}{2}}}; \quad s\in R_+, \\ K_-(s) &= \frac{(1+\lambda^2)^{\frac{1}{2}} \exp\{F_-(s)-\tfrac{1}{4}\pi i\}}{(s-i\delta)^{\frac{1}{2}}}; \quad s\in R_-. \end{aligned}\right\} \tag{A 23}$$

It is readily shown from (A 22) and (A 23) that

$$\left.\begin{aligned} &K_+(s) = K_-(-s); \\ &K_+(s) \sim \frac{\beta_1}{s^{\frac{1}{2}}} \quad \text{as } |s|\to\infty \quad \text{in } R_+; \\ &K_-(s) \sim \frac{\beta_2}{s^{\frac{1}{2}}} \quad \text{as } |s|\to\infty \quad \text{in } R_-, \end{aligned}\right\} \tag{A 24}$$

where β_1 and β_2 are constants. With $K(s)$ defined as in (A 20) we now rewrite (A 17) as

$$J_+(s) = J_-(s); \quad s\in R, \tag{A 25}$$

where

$$\left.\begin{aligned} J_+(s) &= K_+(s)\,\eta_+(s) + \frac{ia}{K_-(-i\delta)(s+i\delta)}; \quad s\in R_+, \\ J_-(s) &= -\frac{\{1-K_-(s)/K_-(-i\delta)\}\,ia}{K_-(s)(s+i\delta)} - \frac{\eta_-(s)}{K_-(s)}; \quad s\in R_-. \end{aligned}\right\} \tag{A 26}$$

From (A 26) it may be seen that J_+ and J_- are analytic in R_+ and R_- respectively with $|J_+(s)|\to 0$, and $|J_-(s)| = o(|s|^{\frac{1}{2}})$ as $|s|\to\infty$ in R_+ and R_- respectively. If we now define $J(s) = J_\pm(s)$, $s\in R_\pm$ then since, from (A 25), $J_-(s)$ is the analytic continuation of $J_+(s)$ into R_-, $J(s)$ is an entire function with $|J(s)| = o(|s|^{\frac{1}{2}})$ as $|s|\to\infty$. It follows, using Liouville's theorem, that $J(s) = a_0$ where a_0 is a constant. If we insist that our solution has the least possible singular behaviour at the pipe orifice, then we require η_+, η_- to decay as rapidly as possible as $|s|\to\infty$. Thus $a_0 = 0$ and (A 26) yields

$$\eta_+(s) = -\frac{ia}{K_-(-i\delta)\,K_+(s)\,(s+i\delta)}; \quad s\in R_+, \tag{A 27a}$$

$$\eta_-(s) = -\frac{ia\{K_-(-i\delta)-K_-(s)\}}{K_-(-i\delta)(s+i\delta)}; \quad s\in R_-, \tag{A 27b}$$

from which we may deduce that $|\eta_+(s)| \sim b_1|s|^{-\frac{1}{2}}$ and $|\eta_-(s)| \sim b_2|s|^{-1}$ as $|s|\to\infty$ in R_+ and R_- respectively, where b_1 and b_2 are constants.

We are now in a position to complete the solution for $\delta \neq 0$. If we make use of (A 12), (A 13), (A 14), (A 16b), (A 18), (A 27), and the Fourier inversion theorem, we find, after some manipulation, that

$$\Phi_0(r,x) = -\frac{ia}{2\pi K_-(-i\delta)} \int_{-\infty}^{\infty} \frac{I_0(\gamma r)\,e^{-isx}\,ds}{K_+(s)\,\gamma I_0'(\gamma)\,(s+i\delta)}; \quad r<1, \tag{A 28}$$

and

$$\Psi_0(r,x) = -\frac{ia\lambda}{2\pi K_-(-i\delta)} \int_{-\infty}^{\infty} \frac{K_0(\gamma r)\,e^{-isx}\,ds}{K_+(s)\,\gamma K_0'(\gamma)\,(s+i\delta)}; \quad r>1. \tag{A 29}$$

From (A 28) and (A 29) it is easily shown that the condition $\lambda\Psi_0(1,0) - \Phi_0(1,0) = a$ is satisfied, which provides a useful check on our solution at this stage.

We next consider in greater detail the solutions (A 28) and (A 29) for $\delta \neq 0$. First we address (A 28) in $x < 0$. It can be shown that the integrand decays exponentially as $|s| \to \infty$ in the upper half-plane, and since $K_+(s)$ is analytic and non-zero in R_+ the only singularities of the integrand in upper half-plane are those of

$$g(\gamma) = \frac{I_0(\gamma r)}{\gamma I_0'(\gamma)}. \tag{A 30}$$

Since g is an even function of γ it is continuous and analytic across the branch cuts for γ in the s-plane, and its only remaining singularities in the upper half-plane are at the roots of $\gamma(s) I_0'\{\gamma(s)\} = 0$. This equation has a countably infinite number of roots, corresponding to simple zeros, in the upper half-plane, at $s = s_n = \mathrm{i}(\mu_n^2 + \delta^2)^{\frac{1}{2}}$, $n = 0, 1, 2, \ldots$. Here the constants μ_n are the positive zeros of $J_1(\mu)$, where J_1 is the Bessel function of the first kind of order one. For $x < 0$ then, the integral (A 28) is evaluated by deforming the contour of integration into the upper half-plane, and using the residue theorem, to give

$$\Phi_0(r, x) = -\frac{a\, \mathrm{e}^{-\delta|x|}}{2\delta^2 K_-^2(-\mathrm{i}\delta)} - \frac{a}{K_-(-\mathrm{i}\delta)} \sum_{n=1}^{\infty} \frac{I_0(\mathrm{i}\mu_n r)\, \mathrm{e}^{-(\mu_n^2+\delta^2)^{\frac{1}{2}}|x|}}{(\mu_n^2+\delta^2)^{\frac{1}{2}}\{(\mu_n^2+\delta^2)^{\frac{1}{2}}+\delta\} K_+\{\mathrm{i}(\mu_n^2+\delta^2)^{\frac{1}{2}}\} I_0''(\mathrm{i}\mu_n)}; \quad r < 1, \quad x < 0. \tag{A 31}$$

Now consider the solution (A 28) in $x > 0$. It is convenient to use (A 18c) and (A 20) to write (A 28) as

$$\Phi_0(r, x) = -\frac{\mathrm{i}a}{2\pi K_-(-\mathrm{i}\delta)} \int_{-\infty}^{\infty} \left[\frac{I_0(\gamma r)\, \gamma K_0'(\gamma) K_-(s)}{\{(1-\lambda^2)\gamma I_0(\gamma) K_0'(\gamma) - \lambda^2\}} - K_-(-\mathrm{i}\delta) \right] \frac{\mathrm{e}^{-\mathrm{i}sx}}{s+\mathrm{i}\delta} \mathrm{d}s - \frac{\mathrm{i}a}{2\pi} \int_{-\infty}^{\infty} \frac{\mathrm{e}^{-\mathrm{i}sx}}{s+\mathrm{i}\delta} \mathrm{d}s. \tag{A 32}$$

Note that in (A 32) we have subtracted, for convenience, the simple pole of the integrand of (A 28) at $s = -\mathrm{i}\delta$. The first integral in (A 32) can now be expressed in a more convenient form by deforming the contour around the branch cut in the lower half-plane, whilst the second integral is readily evaluated via the residue theorem. After considerable manipulation we have

$$\Phi_0(r, x) = \frac{a}{2\pi K_-(-\mathrm{i}\delta)} \int_{\delta}^{\infty} \frac{I_0\{\mathrm{i}\Gamma(p) r\}\, \Gamma(p)\, K_-(-\mathrm{i}p)\, \mathrm{e}^{-px}}{p-\delta} \times \left[\frac{K_0'\{-\mathrm{i}\Gamma(p)\}}{[(1-\lambda^2)\,\mathrm{i}\Gamma(p) I_0\{\mathrm{i}\Gamma(p)\} K_0'\{-\mathrm{i}\Gamma(p)\} + \lambda^2]} - \frac{K_0'\{\mathrm{i}\Gamma(p)\}}{[(1-\lambda^2)\,\mathrm{i}\Gamma(p) I_0\{\mathrm{i}\Gamma(p)\} K_0'\{\mathrm{i}\Gamma(p)\} - \lambda^2]} \right] \mathrm{d}p - a\, \mathrm{e}^{-\delta x}; \quad r < 1, \quad x > 0, \tag{A 33}$$

where $\Gamma(p) = (p+\delta)^{\frac{1}{2}}(p-\delta)^{\frac{1}{2}}$.

We now turn our attention to the solution (A 29) for $r > 1$, with $\delta \neq 0$. The expression (A 29) is in fact a convenient form for the solution. With the integration taking place along the real axis we write $s = \sigma$ and then, with $\gamma(\sigma) = (\sigma^2+\delta^2)^{\frac{1}{2}}$ we have

$$\Psi_0(r, x) = -\frac{\mathrm{i}a\lambda}{2\pi K_-(-\mathrm{i}\delta)} \int_{-\infty}^{\infty} \frac{K_0\{(\sigma^2+\delta^2)^{\frac{1}{2}} r\}\, \mathrm{e}^{-\mathrm{i}\sigma x}\, \mathrm{d}\sigma}{K_+(\sigma)(\sigma^2+\delta^2)^{\frac{1}{2}} K_0'\{(\sigma^2+\delta^2)^{\frac{1}{2}}\}(\sigma+\mathrm{i}\delta)}. \tag{A 34}$$

This completes the solution for $\delta \neq 0$. Our remaining task is to recover the solution of the original harmonic problem via an appropriate limiting process in which $\delta \to 0$.

First, we consider the behaviour of $K_+(s), K_-(s)$ as $\delta \to 0$. It can be shown that both K_+ and K_- remain bounded as $\delta \to 0$ unless $|s| \to 0$ also. For $\delta, |s| \ll 1$ we have the limiting behaviour

$$K_+(s) \sim \frac{\mathrm{i}\sqrt{2}}{s+\mathrm{i}\delta} + C_1, \quad K_-(s) \sim -\frac{\mathrm{i}\sqrt{2}}{s-\mathrm{i}\delta} + C_2 \quad \text{uniformly as } \delta, |s| \to 0, \tag{A 35}$$

where C_1 and C_2 are constants that have not been evaluated explicitly.

For the solution of the original harmonic problem $\hat{\Phi}_0$ is required to satisfy the far-field condition $\nabla\hat{\Phi}_0 \to -\alpha \boldsymbol{i}$ as $x \to -\infty$ in the limit $\delta \to 0$. For non-zero δ we have, from (A 5*a*) and (A 31)

$$\hat{\Phi}_0(r, x) \sim \frac{a}{K_-(-\mathrm{i}\delta)} \left\{ K(-\mathrm{i}\delta)\, \mathrm{e}^{-\delta x} - \frac{\mathrm{e}^{\delta x}}{2\delta^2 K_-(-\mathrm{i}\delta)} \right\} + E_x \quad \text{as } x \to -\infty, \tag{A 36}$$

where E_x denotes terms that remain exponentially small in the limit $x \to -\infty$ as $\delta \to 0$. If we now expand the asymptotic expression (A 36) for $\delta \ll 1$, making use of (A 35), we see that the choice $a = \alpha/2\delta$ gives, in the limit $\delta = 0$,

$$\hat{\Phi}_0(r, x) \sim -\alpha x + \sqrt{2}\alpha C_1 + E_x \quad \text{as } x \to -\infty$$

as required. With this value of a the solution of the original harmonic problem is now determined by taking the limit $\delta \to 0$ in (A 31), (A 33) and (A 34), making use of (A 35).

Consider first the solution in $r < 1$. For $x < 0$ we have from (A 31), (A 5*a*) and (A 1*a*)

$$\tilde{\psi}_0(r, x) = \alpha \left\{ \sqrt{2}C_1 - \frac{1}{\sqrt{2}} \sum_{n=1}^{\infty} \frac{J_0(\mu_n r)\, \mathrm{e}^{-\mu_n |x|}}{\mu_n^2 J_1'(\mu_n) K_+(\mathrm{i}\mu_n)} \right\}, \quad x < 0. \tag{A 37}$$

Similarly we obtain the solution in $x > 0$, via (A 33), as

$$\tilde{\psi}_0(r, x) = \frac{\alpha\lambda^2}{2^{\frac{3}{2}}\pi} \int_0^{\infty} \frac{K_-(\mathrm{i}p) J_0(pr) \{K_0'(\mathrm{i}p) + K_0'(-\mathrm{i}p)\}\, \mathrm{e}^{-px}\, \mathrm{d}p}{\{\lambda^2 + (1-\lambda^2)\,\mathrm{i}pJ_0(p) K_0'(-\mathrm{i}p)\}\{\lambda^2 - (1-\lambda^2)\,\mathrm{i}pJ_0(p) K_0'(\mathrm{i}p)\}} + \alpha x, \quad x > 0. \tag{A 38}$$

For the solution in $r > 1$ we find, from (A 34),

$$\psi_0(r, x) = -\frac{\mathrm{i}\alpha\lambda}{2^{\frac{3}{2}}\pi} \int_{-\infty}^{\infty} \frac{K_0(|\sigma| r)\, \mathrm{e}^{-\mathrm{i}\sigma x}}{\sigma|\sigma| K_+(\sigma) K_0'(|\sigma|)} \mathrm{d}\sigma. \tag{A 39}$$

Finally in this Appendix we determine the asymptotic form that the solutions (A 37)–(A 39) take in the far-field limit. From (A 37) we have immediately

$$\tilde{\psi}_0(r, x) \sim \sqrt{2}\alpha C_1 - \frac{\alpha}{\sqrt{2}} \frac{J_0(\mu_1 r)\, \mathrm{e}^{-\mu_1 |x|}}{\mu_1^2 J_1'(\mu_1) K_+(\mathrm{i}\mu_1)} \quad \text{as } x \to -\infty. \tag{A 40}$$

From (A 38), estimating the integral for large x using Laplace's method, and noting that the integrand takes the value $\pi/\sqrt{2}$ in the limit $p \to 0$, we find

$$\tilde{\psi}_0(r, x) \sim \alpha x + \frac{\alpha\lambda^2}{4x} \quad \text{as } x \to +\infty. \tag{A 41}$$

In $r > 1$ it is appropriate to consider the asymptotic form of the solution (A 39) in the limit $(r^2 + x^2)^{\frac{1}{2}} \to \infty$. The integral may be estimated in that limit, via the method of steepest descents, as

$$\psi_0(r, x) \sim \frac{\alpha\lambda}{4(r^2 + x^2)^{\frac{1}{2}}} \quad \text{as } |x|, r \to \infty. \tag{A 42}$$

In obtaining $\psi_0, \tilde{\psi}_0$ we have chosen the solutions that exhibit the least singular behaviour at the lip of the cylinder as $x \to 0+$. An examination of (A 31), (A 13c, e), in the limit as $\delta \to 0$, shows that this choice leads to the following on $r = 1$ as $x \to 0+$:

$$\frac{\partial \psi_0}{\partial r}, \quad \frac{\partial \tilde{\psi}_0}{\partial r} \sim \gamma_0 \alpha x^{-\frac{1}{2}},$$

where γ_0 is a constant;

$$\frac{\partial \psi_0}{\partial x}, \quad \frac{\partial \tilde{\psi}_0}{\partial x} \quad \text{bounded}.$$

Consequently we have $|\nabla \psi_0|, |\nabla \tilde{\psi}_0| \sim \gamma_0 \alpha x^{-\frac{1}{2}}$ on $r = 1$ as $x \to 0+$.

Appendix B

In this Appendix we turn to the asymmetric components $\psi_2, \tilde{\psi}_2$. These are harmonic functions with boundary conditions set out in (3.24), (3.25) and (3.35). We first write

$$\psi_2(r, \theta, x) = \psi_2^*(r, x) \cos 2\theta, \quad \tilde{\psi}_2(r, \theta, x) = \tilde{\psi}_2^*(r, x) \cos 2\theta, \tag{B 1}$$

and then introduce the new dependent variables

$$\left.\begin{aligned} \hat{\Phi}_2(r, x) &= \tilde{\psi}_2^*(r, x) + \frac{x r^2}{1+\lambda^2}, & r < 1; \\ \hat{\Psi}_2(r, x) &= \psi_2^*(r, x) - \frac{\lambda x}{(1+\lambda^2) r^2}, & r > 1. \end{aligned}\right\} \tag{B 2a, b}$$

The far-field conditions satisfied by $\hat{\Phi}_2, \hat{\Psi}_2$ are

$$\hat{\Phi}_2 \sim \frac{x r^2}{1+\lambda^2} \quad \text{as } x \to -\infty, \quad \hat{\Phi}_2 \to 0 \quad \text{as } x \to \infty, \quad r < 1, \tag{B 3a, b}$$

$$\hat{\Psi}_2 \sim -\frac{\lambda x}{(1+\lambda^2) r^2} \quad \text{as } x \to -\infty, \quad \hat{\Psi}_2 \to 0 \quad \text{as } x \to \infty, \quad r > 1, \tag{B 3c, d}$$

with the remaining conditions, on $r = 1$, given as

$$\frac{\partial \hat{\Phi}_2}{\partial r} = \frac{2x}{1+\lambda^2}, \quad \frac{\partial \hat{\Psi}_2}{\partial r} = \frac{2\lambda x}{1+\lambda^2}, \quad x < 0, \tag{B 4a, b}$$

$$\frac{\partial \hat{\Psi}_2}{\partial r} = \lambda \frac{\partial \hat{\Phi}_2}{\partial r}, \quad \lambda \frac{\partial \hat{\Psi}_2}{\partial x} = \frac{\partial \hat{\Phi}_2}{\partial x}, \quad x > 0. \tag{B 4c, d}$$

As in Appendix A, in order to employ the Wiener–Hopf technique, we solve a modified Helmholtz problem in which $\hat{\Phi}_2$ and $\hat{\Psi}_2$ satisfy

$$\Delta^2 \hat{\Phi}_2 - \frac{4}{r^2} \hat{\Phi}_2 - \delta^2 \hat{\Phi}_2 = 0, \quad r < 1, \tag{B 5a}$$

$$\Delta^2 \hat{\Psi}_2 - \frac{4}{r^2} \hat{\Psi}_2 - \delta^2 \hat{\Psi}_2 = 0, \quad r > 1, \tag{B 5b}$$

This modified problem also requires a modification of the boundary conditions (B 3a,c), (B 4a,b) which become, respectively,

$$\hat{\Phi}_2 \sim -\frac{r^2}{2\delta(1+\lambda^2)}(e^{-\delta x}-e^{\delta x}) \quad \text{as } x\to-\infty \quad \text{for } r<1, \tag{B 6a}$$

$$\hat{\Psi}_2 \sim \frac{\lambda}{2\delta(1+\lambda^2)r^2}(e^{-\delta x}-e^{\delta x}) \quad \text{as } x\to-\infty \quad \text{for } r>1, \tag{B 6b}$$

and

$$\frac{\partial\hat{\Phi}_2}{\partial r}=-\frac{1}{\delta(1+\lambda^2)}(e^{-\delta x}-e^{\delta x}), \quad \frac{\partial\hat{\Psi}_2}{\partial r}=-\frac{\lambda}{\delta(1+\lambda^2)}(e^{-\delta x}-e^{\delta x}), \tag{B 7a,b}$$

on $r=1$ in $x<0$. Note that the original boundary conditions are recovered in the limit $\delta\to 0$. To complete the formulation of the problem it can be shown that as $x\to\infty$

$$\hat{\Phi}_2 \sim d_1\frac{e^{-\delta x}}{x} \quad \text{in } r<1; \quad \hat{\Psi}_2 \sim d_2\frac{e^{-\delta\hat{R}}}{\hat{R}} \quad \text{in } r>1,$$

where d_1 and d_2 are constants.

The exponentially growing parts of (B 6a,b) are removed by introducing the functions Φ_2,Ψ_2 such that

$$\Phi_2=\hat{\Phi}_2+\frac{r^2}{2\delta(1+\lambda^2)}e^{-\delta x} \quad \text{in } r<1, \tag{B 8a}$$

$$\Psi_2=\hat{\Psi}_2-\frac{\lambda}{2\delta(1+\lambda^2)r^2}e^{-\delta x} \quad \text{in } r>1. \tag{B 8b}$$

Equations (B 5a,b) are satisfied by Φ_2,Ψ_2 respectively whilst from (B 4d) and (B 7a,b) we have

$$\lambda\frac{\partial\Psi_2}{\partial x}-\frac{\partial\Phi_2}{\partial x}=\frac{1}{2}e^{-\delta x} \quad \text{on } r=1 \quad \text{in } x>0, \tag{B 9a}$$

$$\frac{\partial\Phi_2}{\partial r}=\frac{1}{\delta(1+\lambda^2)}e^{\delta x}, \quad \frac{\partial\Psi_2}{\partial r}=\frac{\lambda}{\delta(1+\lambda^2)}e^{\delta x} \quad \text{on } r=1 \quad \text{in } x<0. \tag{B 9b,c}$$

Furthermore it may now be shown that

$$|\Phi_2| \sim A_2 e^{-\delta|x|}, \quad |\Psi_2| \sim B_2 e^{-\delta|x|} \quad \text{as } |x|\to\infty, \tag{B 10}$$

where A_2, B_2 are constants.

Since (B 10) ensures exponential decay the Wiener–Hopf technique may be employed. The full-range and half-range Fourier transforms of Φ_2 and Ψ_2 are defined as for the corresponding quantities in Appendix A. Again, full-range transforms are analytic in R whilst '+' and '−' transforms are analytic in R_+ and R_- respectively, with all transforms exhibiting algebraic decay as $|s|\to\infty$ in the appropriate domain of definition.

If we follow the procedures adopted in Appendix A we obtain, for the full-range transforms $\bar{\varphi}_2,\bar{\psi}_2$ of Φ_2 and Ψ_2,

$$\left.\begin{aligned}\bar{\varphi}_2(r,s)&=\bar{A}(s)I_2(\gamma R), \quad s\in R, \quad r<1,\\ \bar{\psi}_2(r,s)&=\bar{B}(s)K_2(\gamma R), \quad s\in R, \quad r>1,\end{aligned}\right\} \tag{B 11}$$

where I_2 and K_2 are modified Bessel functions of order two and $\bar{A}(s)$, $\bar{B}(s)$ are, as yet, undetermined functions.

If we transform the boundary conditions (B 4*c*), (B 9) and eliminate $\bar{A}(s)$, $\bar{B}(s)$, the following Wiener–Hopf equation results:

$$\bar{K}(s)\,\bar{\eta}_+ + \bar{\eta}_- = \frac{\mathrm{i}}{2\delta(s+\mathrm{i}\delta)} + \frac{\mathrm{i}\bar{K}(s)}{(1+\lambda^2)\,\delta(s-\mathrm{i}\delta)}, \quad s \in R, \tag{B 12}$$

where

$$\bar{\eta}_+ = \left.\frac{\partial \bar{\varphi}_{2+}}{\partial r}\right|_{r=1}, \quad \bar{\eta}_- = \lambda\bar{\psi}_{2-}|_{r=1} - \bar{\varphi}_{2-}|_{r=1},$$

and

$$\bar{K}(s) = \frac{I_2(\gamma)\,K_2'(\gamma) - \lambda^2 K_2(\gamma)\,I_2'(\gamma)}{\gamma I_2'(\gamma)\,K_2'(\gamma)}. \tag{B 13}$$

Again, for λ close to unity, an application of Rouché's theorem shows that $\bar{K}(s)$ is non-zero in the entire cut s-plane.

The solution of the Wiener–Hopf equation is given by

$$\left.\begin{aligned} \bar{\eta}_+(s) &= \frac{\mathrm{i}\{\bar{K}_+(s) - \bar{K}_+(\mathrm{i}\delta)\}}{(1+\lambda^2)\,\delta\bar{K}_+(s)\,(s-\mathrm{i}\delta)} + \frac{\mathrm{i}}{2\delta\bar{K}_+(s)\,\bar{K}_-(-\mathrm{i}\delta)\,(s+\mathrm{i}\delta)}, && s \in R_+, \\ \bar{\eta}_-(s) &= -\frac{\mathrm{i}\{\bar{K}_-(s) - \bar{K}_-(-\mathrm{i}\delta)\}}{2\delta\bar{K}_-(-\mathrm{i}\delta)\,(s+\mathrm{i}\delta)} + \frac{\mathrm{i}\bar{K}_+(\mathrm{i}\delta)\,\bar{K}_-(s)}{(1+\lambda^2)\,\delta(s-\mathrm{i}\delta)}, && s \in R_-. \end{aligned}\right\} \tag{B 14}$$

In (B 14) $\bar{K}_+(s)$, $\bar{K}_-(s)$ are the multiplicative factors of the kernel $\bar{K}(s)$ and may be expressed, through the Cauchy integrals, as

$$\bar{K}_\pm(s) = \frac{(1+\lambda^2)^{\frac{1}{2}}\exp\{\pm\frac{1}{4}\pi\mathrm{i} + F_\pm(s)\}}{(s\pm\mathrm{i}\delta)^{\frac{1}{2}}}, \quad s \in R_\pm, \tag{B 15}$$

where

$$F_\pm(s) = \pm\frac{1}{2\pi\mathrm{i}}\int_{C_\pm} \frac{\log\left\{\dfrac{\gamma(\omega)\,\bar{K}(\omega)}{1+\lambda^2}\right\}}{\omega - s}\,\mathrm{d}\omega \tag{B 16}$$

with the contours of integration C_+, C_- as in Appendix A.

We may now obtain the solutions in $r \gtrless 1$ for $\delta \neq 0$ by making use of (B 14) and the Fourier inversion theorem.

For $r < 1$ the solution in $x < 0$ is obtained by deforming the contour into the upper half-plane to give:

$$\begin{aligned} \Phi_2(r,x) = \frac{r^2\,\mathrm{e}^{\delta x}}{2\delta^2(1+\lambda^2)} + \sum_{n=1}^{\infty}\Bigg[&\frac{1}{2\bar{K}_-(-\mathrm{i}\delta)\{(\Omega_n^2+\delta^2)^{\frac{1}{2}}+\delta\}} \\ &- \frac{\bar{K}_+(\mathrm{i}\delta)}{(1+\lambda^2)\{(\Omega_n^2+\delta^2)^{\frac{1}{2}}-\delta\}}\Bigg]\frac{I_2(\mathrm{i}\Omega_n r)\,\mathrm{e}^{(\Omega_n^2+\delta^2)^{\frac{1}{2}}x}}{\bar{K}_+\{\mathrm{i}(\Omega_n^2+\delta^2)^{\frac{1}{2}}\}\,I_2''(\mathrm{i}\Omega_n)\,(\Omega_n^2+\delta^2)^{\frac{1}{2}}}, \\ &\text{for } r<1 \quad \text{in } x<0, \end{aligned} \tag{B 17}$$

where the Ω_n represent the positive zeros of $J_2'(\Omega)$.

For $x > 0$ the solution is obtained, by deforming the contour around the branch cut for γ in the lower half-plane, as

$$\begin{aligned} \Phi_2(r,x) = \frac{\mathrm{i}}{2\pi\delta}\int_{p=\delta}^{\infty} \hat{K}(p)\,I_2\{\mathrm{i}\Gamma(p)\,r\}\,\bar{K}_-(\mathrm{i}p)\left\{\frac{\bar{K}_+(\mathrm{i}\delta)}{(1+\lambda^2)\,(p+\delta)} - \frac{1}{2\bar{K}_-(-\mathrm{i}\delta)\,(p-\delta)}\right\}\mathrm{e}^{-px}\,\mathrm{d}p \\ + \frac{r^2\,\mathrm{e}^{-\delta x}}{2\delta(1+\lambda^2)} \quad \text{for } r<1 \quad \text{in } x>0, \end{aligned} \tag{B 18}$$

where

$$\hat{K}(p) = \left[\frac{K_2'\{-\mathrm{i}\Gamma(p)\}}{[I_2\{\mathrm{i}\Gamma(p)\}K_2'\{-\mathrm{i}\Gamma(p)\}+\lambda^2 K_2\{-\mathrm{i}\Gamma(p)\}I_2'\{\mathrm{i}\Gamma(p)\}]} - \frac{K_2'\{\mathrm{i}\Gamma(p)\}}{[I_2\{\mathrm{i}\Gamma(p)\}K_2'\{\mathrm{i}\Gamma(p)\}-\lambda^2 K_2\{\mathrm{i}\Gamma(p)\}I_2'\{\mathrm{i}\Gamma(p)\}]}\right], \quad \text{(B 19)}$$

and $\Gamma(p)$ is as defined in Appendix A.

For $r > 1$ the most convenient form of the solution is obtained as

$$\Psi_2(r,x) = \frac{\mathrm{i}\lambda}{2\pi\delta}\left[\int_{-\infty}^{\infty}\left\{\frac{K_2(\gamma r)}{2\bar{K}_-(-\mathrm{i}\delta)\bar{K}_+(s)\gamma K_2'(\gamma)(s+\mathrm{i}\delta)}+\frac{1}{2(1+\lambda^2)r^2(s+\mathrm{i}\delta)}\right.\right.$$
$$\left.\left.-\frac{K_2(\gamma r)\bar{K}_+(\mathrm{i}\delta)}{(1+\lambda^2)\bar{K}_+(s)\gamma K_2'(\gamma)(s-\mathrm{i}\delta)}-\frac{1}{2(1+\lambda^2)r^2(s-\mathrm{i}\delta)}\right\}\mathrm{e}^{-\mathrm{i}sx}\,\mathrm{d}s\right.$$
$$\left.+\frac{1}{2(1+\lambda^2)r^2}\int_{-\infty}^{\infty}\frac{\mathrm{e}^{-\mathrm{i}sx}}{s-\mathrm{i}\delta}\mathrm{d}s-\frac{1}{2(1+\lambda^2)r^2}\int_{-\infty}^{\infty}\frac{\mathrm{e}^{-\mathrm{i}sx}}{s+\mathrm{i}\delta}\mathrm{d}s\right]. \quad \text{(B 20)}$$

We are now in a position to recover the solution of the original harmonic problem by taking the limit $\delta \to 0$ in (B 17)–(B 20). First note, from (B 15) that

$$\bar{K}_\pm(s) \sim \left(\frac{1+\lambda^2}{2}\right)^{\frac{1}{2}} \quad \text{as } \delta, |s| \to 0. \quad \text{(B 21)}$$

If we now make use of (B 2), (B 8), (B 17)–(B 21) and allow $\delta \to 0$ we obtain, after considerable manipulation, the solution of the original harmonic problem. Thus for $r < 1$ we have

$$\tilde{\psi}_2^*(r,x) = \left(\frac{2}{1+\lambda^2}\right)^{\frac{1}{2}}\sum_{n=1}^{\infty}(1+A\Omega_n)\frac{J_2(\Omega_n r)\,\mathrm{e}^{-\Omega_n|x|}}{\Omega_n^3\bar{K}_+(\mathrm{i}\Omega_n)J_2''(\Omega_n)} \quad \text{in } x<0, \quad \text{(B 22}a\text{)}$$

and

$$\tilde{\psi}_2^*(r,x) = -\frac{xr^2}{1+\lambda^2}-\frac{\mathrm{i}}{\pi\{2(1+\mathrm{l}^2)\}^{\frac{1}{2}}}\int_0^{\infty}\hat{K}(p)\frac{J_2(pr)}{p^2}\bar{K}_-(-\mathrm{i}p)\,\mathrm{e}^{-px}(1-Ap)\,\mathrm{d}p \quad \text{in } x>0, \quad \text{(B 22}b\text{)}$$

where $\hat{K}(p)$ is defined in (B 19) and

$$A = \left\{\int_0^{\infty}\frac{\hat{K}(p)J_2'(p)\bar{K}_+(\mathrm{i}p)}{p}\right\}\mathrm{d}p\left\{\int_0^{\infty}\left[\hat{K}(p)J_2'(p)\bar{K}_+(\mathrm{i}p)-\frac{2\mathrm{i}}{(1+\lambda^2)^{\frac{1}{2}}p^{\frac{1}{2}}}\right]\mathrm{d}p\right\}^{-1}$$

is a constant.

The corresponding solutions for $r > 1$ are given by

$$\psi_2^*(r,x) = \frac{-\lambda}{\pi\{2(1+\lambda^2)\}^{\frac{1}{2}}}\int_0^{\infty}\left\{\frac{K_2(\mathrm{i}pr)}{K_2'(\mathrm{i}p)}+\frac{K_2(-\mathrm{i}pr)}{K_2'(-\mathrm{i}p)}\right\}\frac{\mathrm{e}^{-p|x|}}{p^3\bar{K}_+(\mathrm{i}p)}(1+Ap)\,\mathrm{d}p \quad \text{in } x<0, \quad \text{(B 23}a\text{)}$$

and

$$\psi_2^*(r,x) = \frac{\lambda x}{(1+\lambda^2)r^2}-\frac{\lambda}{\pi\{2(1+\lambda^2)\}^{\frac{1}{2}}}$$
$$\times\int_0^{\infty}\left[\frac{\mathrm{i}K_2(\mathrm{i}pr)}{\{I_2(\mathrm{i}p)K_2'(\mathrm{i}p)-\lambda^2K_2(\mathrm{i}p)I_2'(\mathrm{i}p)\}}+\frac{\mathrm{i}K_2(-\mathrm{i}pr)}{\{I_2(\mathrm{i}p)K_2'(-\mathrm{i}p)+\lambda^2K_2(-\mathrm{i}p)I_2'(\mathrm{i}p)\}}\right]$$
$$\times\frac{\bar{K}_-(-\mathrm{i}p)I_2'(\mathrm{i}p)}{p^2}\mathrm{e}^{-px}(1-Ap)\,\mathrm{d}p \quad \text{in } x>0. \quad \text{(B 23}b\text{)}$$

In this Appendix we finally evaluate the asymptotic forms of the solutions (B 22), (B 23) in the limits $x \to \pm\infty$.

For $r < 1$ we have, immediately, from (B 22a)

$$\tilde{\psi}_2^*(r,x) \sim \left(\frac{2}{1+\lambda^2}\right)^{\frac{1}{2}} (1+A\Omega_1)\frac{J_2(\Omega_1 r)\,\mathrm{e}^{-\Omega_1|x|}}{\Omega_1^3 \bar{K}_+(\mathrm{i}\Omega_1) J_2''(\Omega_1)} \quad \text{as } x \to -\infty, \tag{B 24}$$

whilst an application of Laplace's method to (B 22b) yields

$$\tilde{\psi}_2^*(r,x) \sim -\frac{xr^2}{1+\lambda^2}\left(1-\frac{\lambda^2}{8(1+\lambda^2)x^4}\right) \quad \text{as } x \to +\infty. \tag{B 25}$$

For $r > 1$ we use Laplace's method to obtain the asymptotic forms of (B 23) as

$$\psi_2^*(r,x) \sim -\frac{\lambda(r^2+r^{-2})}{16(1+\lambda^2)x^2} \quad \text{as } x \to -\infty, \tag{B 26}$$

and

$$\psi_2^*(r,x) \sim \frac{\lambda x}{(1+\lambda^2)r^2}\left\{1+\frac{(1-\lambda^2)(1+\lambda^2)^{-1}+r^4}{16x^4}\right\} \quad \text{as } x \to +\infty, \tag{B 27}$$

where it should be noted that the limits in (B 26) and (B 27) are taken with r fixed and finite.

As in Appendix A, we have chosen here the solutions ψ_2^*, $\tilde{\psi}_2^*$ that have the least possible singular behaviour as $x \to 0+$ at the lip of the cylinder. From (B 14) and (B 22b) we find that this choice leads to the following as $x \to 0+$ on $r = 1$:

$$\frac{\partial\tilde{\psi}_2^*}{\partial r} \sim -\frac{\sqrt{2A}}{(1+\lambda^2)\pi^{\frac{1}{2}}}x^{-\frac{1}{2}}, \quad \frac{\partial\psi_2^*}{\partial r} \sim -\frac{\sqrt{2\lambda A}}{(1+l^2)\pi^{\frac{1}{2}}}x^{-\frac{1}{2}}, \quad \frac{\partial\psi_2^*}{\partial x}, \quad \frac{\partial\tilde{\psi}_2^*}{\partial x} \quad \text{bounded.}$$

The implications of the singular behaviour at the lip are discussed in §4.

REFERENCES

Chang, H. C. 1942 Aufrollung eines zylindrischen Strahles durch Querwind. Dissertation, University of Göttingen. (Translated as ARL-73-0131, 1973.)

Lennox, S. C. & Pack, D. C. 1963 The flow in compound jets. *J. Fluid Mech.* **15**, 513–526.

McGuirk, J. J. & Rodi, W. 1979 Mathematical modelling of three-dimensional heated surface jets. *J. Fluid Mech.* **95**, 609–633.

Sykes, R. I., Lewellen, W. S. & Parker, S. F. 1986 On the vorticity dynamics of a turbulent jet in a crossflow. *J. Fluid Mech.* **168**, 393–413.